

ESD ACCESSION LIST

ESTI Call No. **AL 57858**

Copy No. 1 of 2 cys.

Technical Note

1967-43

Hall Coefficient
and

Transverse Magnetoresistance
in HgTe at 4.2°K and 77°K

T. C. Harman
J. M. Honig
P. H. Trent

25 August 1967

Prepared under Electronic Systems Division Contract AF 19(628)-5167 by

Lincoln Laboratory

MASSACHUSETTS INSTITUTE OF TECHNOLOGY

Lexington, Massachusetts



ADD 458055

The work reported in this document was performed at Lincoln Laboratory, a center for research operated by Massachusetts Institute of Technology, with the support of the U.S. Air Force under Contract AF 19(628)-5167.

This report may be reproduced to satisfy needs of U.S. Government agencies.

This document has been approved for public release and sale; its distribution is unlimited.

MASSACHUSETTS INSTITUTE OF TECHNOLOGY
LINCOLN LABORATORY

HALL COEFFICIENT AND TRANSVERSE MAGNETORESISTANCE
IN HgTe AT 4.2°K AND 77°K

T. C. HARMAN

J. M. HONIG

Group 85

P. H. TRENT

Group 81

TECHNICAL NOTE 1967-43

25 AUGUST 1967

ABSTRACT

A band structure model is proposed in Fig. 1(d) which is consistent with magneto-Hall and magnetoresistance data obtained for various samples of HgTe at 4.2°K. Using an optimization routine it was ascertained that the data could be fitted on the basis of a three-carrier model involving two sets of electrons and one set of holes. Under special crystal growth conditions the electron Hall mobility at 4.2°K of HgTe exceeded 640,000 cm²/v-sec.

Accepted for the Air Force
Franklin C. Hudson
Chief, Lincoln Laboratory Office

CONTENTS

Abstract	iii
Introduction	1
Preparation of Materials	6
Experimental Results	7
Analysis of Results	7
Conclusions	16
APPENDIX A – The Quartic Band	17
APPENDIX B – Optimization Routine	22
References	24

Hall Coefficient and Transverse Magnetoresistance in HgTe at 4.2°K and 77°K

Introduction

While much work has been published in the last few years pertaining to the thermoelectric, thermomagnetic, and optical properties of HgTe, there is as yet no unanimity of opinion concerning the details of the band structure of this material. In 1961, it was concluded⁽¹⁾ that HgSe and HgSe_{0.5}Te_{0.5} are semimetals and it was suggested that HgTe might be likewise. This was later corroborated in measurements of the Hall coefficient and of electrical resistivity⁽²⁾ on HgTe and on its alloys, at low concentration, with CdTe. These and related experiments were ultimately interpreted⁽³⁾ in terms of a band structure model derived from that proposed originally by Groves and Paul⁽⁴⁾ for grey tin. As illustrated in Fig. 1(a), the band structure normally encountered in Group IV elements involves a Γ_6 conduction band separated by a set of Γ_8 bands that are degenerate at the origin. The dispersion relations for grey tin are shown in Fig. 1(b) in terms of the Γ_8 bands lying above the Γ_6 band; relative to the diamond structure, the order of the bands is now inverted.

The success of the band inversion procedure in explaining the semimetallic properties of grey tin suggests that a similar scheme might be tried for HgTe. The parent band structure in

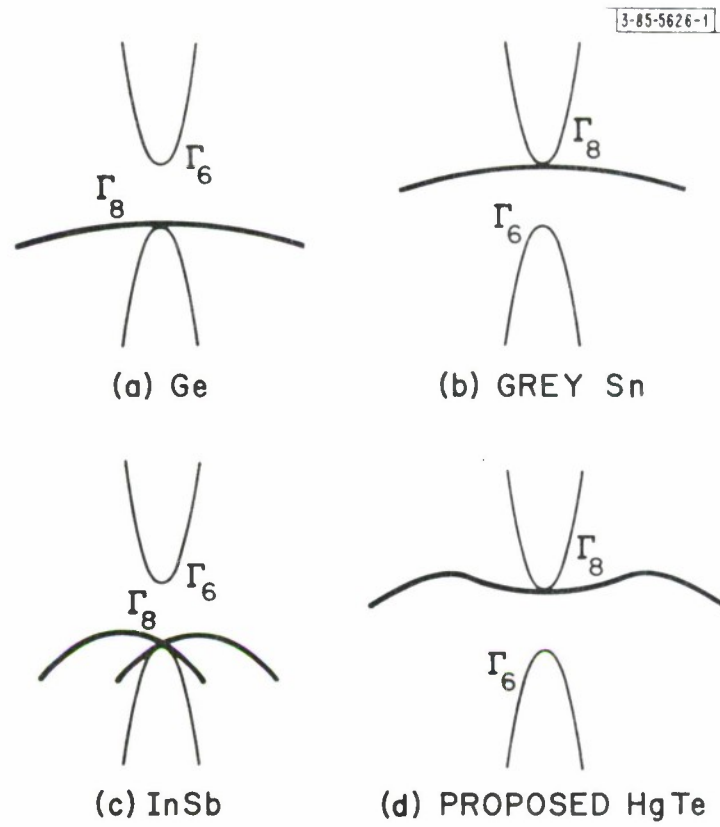


Fig. 1. Various band structure models.

this case, which corresponds to the zinc blende crystal structure, is shown in Fig. 1(c) and is labelled as the InSb structure. Owing to lack of inversion symmetry, the energy dispersion relations now contain a term linear to the wave number vector, \vec{k} . As a consequence, a small split is predicted, away from $\vec{k} = 0$, in the Γ_8 band of Fig. 1(c), with shallow extrema located away from the origin of the Brillouin zone. Apparently, this deviation from (1a) is so slight that it has not been observed, even in InSb, experimentally. The problem of inverting the InSb model has been considered by Gorzkowski⁽⁵⁾, who indicates that a quantitative specification of $\epsilon(\vec{k})$ would be a complex undertaking. In the absence of a simple quantitative theoretical inversion scheme, we therefore propose a band structure model for HgTe in Fig. 1(d) that is consistent with our experimental results.

If Fig. 1(b) represents the band structure of HgTe, then it should be possible to explain all electrical measurements, down to liquid helium temperatures, in terms of one set of holes and one set of electrons, so long as the Fermi level remains close to the degenerate band edge energy. By contrast, the model represented by Fig. 1(d) predicts that two sets of electrons and one set of holes participate in conduction processes under these conditions. This point is brought out in Appendix A.

The interpretation of experimental results with respect to this problem is still rather confused: In a review⁽⁶⁾ of

work completed through 1964, it was pointed out that a two-carrier model is inadequate to account for the transverse magnetoresistance and magneto-Hall data measurements at 77°K and 4.2°K for a variety of doping levels, and this was attributed to an unusually complex valence band structure. More recent work has furnished further corroboration: Ivanov-Omskii and co-workers⁽⁷⁾ have reported systematic measurements on a series of samples which varied over a wide range of net donor and acceptor concentration. Their attempts to fit the data to a two-carrier model, using the method of Hilsum and Barrie⁽⁸⁾ proved unsuccessful. By contrast, Stradling and Antcliffe⁽⁹⁾ have reported quantum oscillations in magnetoresistance at 4.2°K in high magnetic fields on a sample of HgTe in which the Hall coefficient reversed sign with increasing magnetic field. They interpreted their results in terms of a two-carrier model and they report an overlap energy in excess of 0.0007 eV between the valence and conduction bands. No attempt was made to determine if their data were also consistent with a three-carrier model at low temperatures. Delves⁽¹⁰⁾ investigated the properties of single crystals of $\text{Hg}_{1-x}\text{Mn}_x\text{Te}$; from measurements at 77°K for small x he provisionally identified a second set of electron-like carriers. On the other hand, Tovstyuk and co-workers⁽¹¹⁾ concluded that their measurements indicated the presence of one set of electrons and two sets of holes in their samples.

Kolosov and Sharavskii⁽¹²⁾ reach a similar conclusion on the basis of Seebeck coefficient measurements at 188°K in a transverse magnetic field. Verié⁽¹³⁾ bases the interpretation of his electrical measurements in the range 77 - 373°K on a two-band model, though he does sketch an overlap band model similar to that in Fig. 1(d). Finally, Yamamoto and Fukuroi⁽¹⁴⁾ on the basis of the Shubnikov-de Haas effect conclude that HgTe is characterized by two distinct conduction bands involving electrons of different mass.

Part of the difficulty in arriving at a clear decision concerning the applicability of the various band structures stems from the fact that a three-carrier model yields very complex expressions for the transport coefficients⁽¹⁵⁾, so that it becomes difficult to make comparisons between theoretical predictions and experimental observations. The present work was undertaken to clarify aspects concerning the applicability of the three-carrier model to HgTe. Towards this end we accumulated a large body of experimental results on the Hall coefficient and the magnetoresistance of undoped HgTe. Selected representative runs were then subjected to optimal fitting procedures by a computer to ascertain whether a three-carrier model was indeed required to fit the data, and if so, whether one could distinguish between the alternatives of requiring two sets of electrons and one set of holes as against the inverse possibility.

Preparation of Materials

The three samples reported on in this investigation were prepared by the technique discussed in Ref. 5 with the following differences in detail: Sample 4A was an as-grown sample cut from the first-to-freeze part of an ingot grown at a rate of 3 mm/hr from a stoichiometric 100 gm charge which had been sealed, along with 2.7 mg of Al, in a quartz tube. The temperature of the coolest part of the tube in contact with vapor during growth was 560°C, corresponding to a mercury pressure of 15 atm. Sample 300-2A was cut from the first-to-freeze part of an ingot grown at a rate of 3 mm/hr, from a stoichiometric 400 gm charge containing 10.8 gms of excess Hg. The temperature of the coolest part of the tube in contact with vapor during growth was 590°C. The as-grown sample was sealed in an evacuated quartz tube and the tube placed in the first zone at a temperature of 350°C, while the temperature of the coolest part or second zone was 300°C. The sample was annealed for 336 hrs and quenched in water. Sample 50 LB was cut 3 mm from the first-to-freeze part of an ingot, which was grown from a stoichiometric 400 gm charge containing 15 gms of excess Hg. The growth rate was 0.1 mm/hr, and the material was quenched in water. The temperature of the coolest part of the tube in contact with vapor during growth was 590°C. Since only 10 gm of excess Hg was required to make up for the loss of mercury to the vapor, this ingot crystallized from a liquid composition that was slightly rich in mercury.

Experimental Results

Representative data for the Hall coefficient in low magnetic field, for the electrical resistivity in the absence of magnetic fields, for transverse magnetoresistance, and for Hall mobility at 300, 77 and 4.2°K are assembled in Table 1. An interesting feature of the data is the unusually large value of the electron Hall mobility of unannealed sample 50 LB at 4.2°K. The value of 640,000 cm²/volt-sec is significantly higher than the previously higher value of 360,000 cm²/volt-sec reported in Ref. 6. In fact, unannealed specimens from ingot 50 have exhibited unusually well defined quantum oscillatory effects in both magnetoresistance and magneto-optical measurements.⁽¹⁶⁾

Analysis of Results

The magneto-Hall and magnetoresistance measurements taken at 77°K and 4.2°K were first analyzed according to the method of Hilsum and Barrie.⁽⁸⁾ Plots were made of the Hall coefficients vs magnetoresistance and of the magneto-Hall and magnetoresistance vs the inverse square magnetic field. These should result in straight lines on the basis of a two-carrier model; they were, in fact, found to exhibit serious departures from linearity. This clearly required a more sophisticated analysis in terms of at least a three-carrier model.

The transport theory involving such a model was first worked out by Willardson and co-workers⁽¹⁷⁾ for the case of

TABLE 1

Experimental Values of some Electrical Properties of HgTe Samples

Sample	Dopant	300°K		77°K		4.2°K	
		(1)	(2)	(1)	(2)	(1)	(2)
50 LB	None			-94	9.6×10^{-4}	10.7	-2700
300-2A	None			-99	2.1×10^{-3}	5.9	-1210
4A	Al	-27	1.95×10^{-3}	-14.5	1.29×10^{-2}	0.137	-4.2
							1.43×10^{-2}
							0.076

(1) Hall coefficient \mathcal{C} ($\text{cm}^3 \text{C}^{-1}$) at $H = 4$ kG at 300°K and 77°K and $H = 0.4$ kG at 4.2°K.(2) Electrical resistivity in zero magnetic field, $\rho(0)$ (ohm-cm).(3) Transverse magnetoresistance, $\Delta\rho/\rho(0)$, at $H = 21$ kG.(4) Hall mobility, $\mathcal{C}/\rho(0)$, at $H = 0.4$ kG.

p-type Ge. The final results rested on two assumptions, namely that classical statistics was applicable and that the mean free path of the charge carriers was independent of energy. Even so, the final results were rather complex, involving exponential integrals and error functions. In HgTe the situation is further complicated by the fact that for semimetals classical statistics is inapplicable. Accordingly, it was decided to adopt a thermodynamic formulation⁽¹⁵⁾ for isotropic materials in which the overall conductivity σ and Hall coefficient R are expressed in terms of the one-band contributions σ_i and R_i ($i = 1, 2, 3$). That these relations should apply to HgTe is substantiated by unpublished work of the authors on the angular dependence of magnetoresistance of oriented single crystals of HgTe in high magnetic fields; no significant anisotropy effects were encountered even in the mixed conduction region.

For ease of interpretation, the substitutions $\sigma_i = n_i e \mu_i$ and $R_i = 1/n_i e$ were used in the overall expressions for R and σ . Here, e is the electronic charge, n_i the carrier density, and μ_i the carrier mobility of the i th species. In adopting these expressions we neglect the variation of R_i with the magnetic field, H , which is usually considerably less than the maximum value of 50%. We also neglect the dependence of σ_i on H , which is usually considerably less than the maximum factor of 2.4.^(18,20) Since changes in R and σ of many orders of magnitude are observed,

TABLE 2

Calculated Carrier Concentrations and Carrier Mobilities in HgTe at 4.2°K

Sample No.	$n_1 (\text{cm}^{-3})$	$n_2 (\text{cm}^{-3})$	$n_3 (\text{cm}^{-3})$	$\mu_1 (\text{cm}^2/\text{v-sec})$	$\mu_2 (\text{cm}^2/\text{v-sec})$	$\mu_3 (\text{cm}^2/\text{v-sec})$
50 LB	-2.1×10^{15}	-7.0×10^{15}	6.2×10^{14}	-6.5×10^5	-9.5×10^2	7.1×10^4
300-2A	-1.2×10^{15}	-3.3×10^{15}	6.4×10^{16}	-1.0×10^5	-1.3×10^4	420
4A	-1.2×10^{15}	-1.0×10^{16}	2.5×10^{18}	-1.2×10^4	-1.7×10^3	160

it is believed that the conclusions reached in this publication are not altered by use of these simplifications.

As Fischer⁽¹⁹⁾ was first to show, in the approximation scheme discussed above, the dependence of the overall resistivity ρ and of the overall Hall coefficient \mathcal{R} on H may be expressed as

$$\rho(x) = \frac{1}{e} \frac{A + Bx + Lx^2}{A^2 + Dx + Mx^2} \quad (1)$$

$$\mathcal{R}(x) = \frac{1}{e} \frac{E + Fx + Nx^2}{A^2 + Dx + Mx^2} \quad (2)$$

where, with e in coulombs, $x \equiv 10^{-8}H^2$ (H in gauss), and where $A, B, D, E, F, L, M,$ and N are eight nonlinear functions of the three charge carrier densities n_i (in cm^{-3}) and of the three mobilities μ_i (in $\text{cm}^2/\text{volt-sec}$) participating in conduction.

The parameters n_i and μ_i were determined with the aid of a computer program described in further detail in Appendix B. In essence, the experimentally determined $\rho(0)$ and $\mathcal{R}(H_\ell)$ were used as input variables for a program which yielded values of n_i and μ_i that provided an optimal fit of Eq.(2) to the experimental Hall measurements. With the n_i and μ_i determined in this manner, the magnetoresistance was then calculated from Eq.(1) according to the relation $\rho(H)/\rho(0)-1$.

The parameters determined in this fashion for three representative specimens are listed in Table 2. The following points

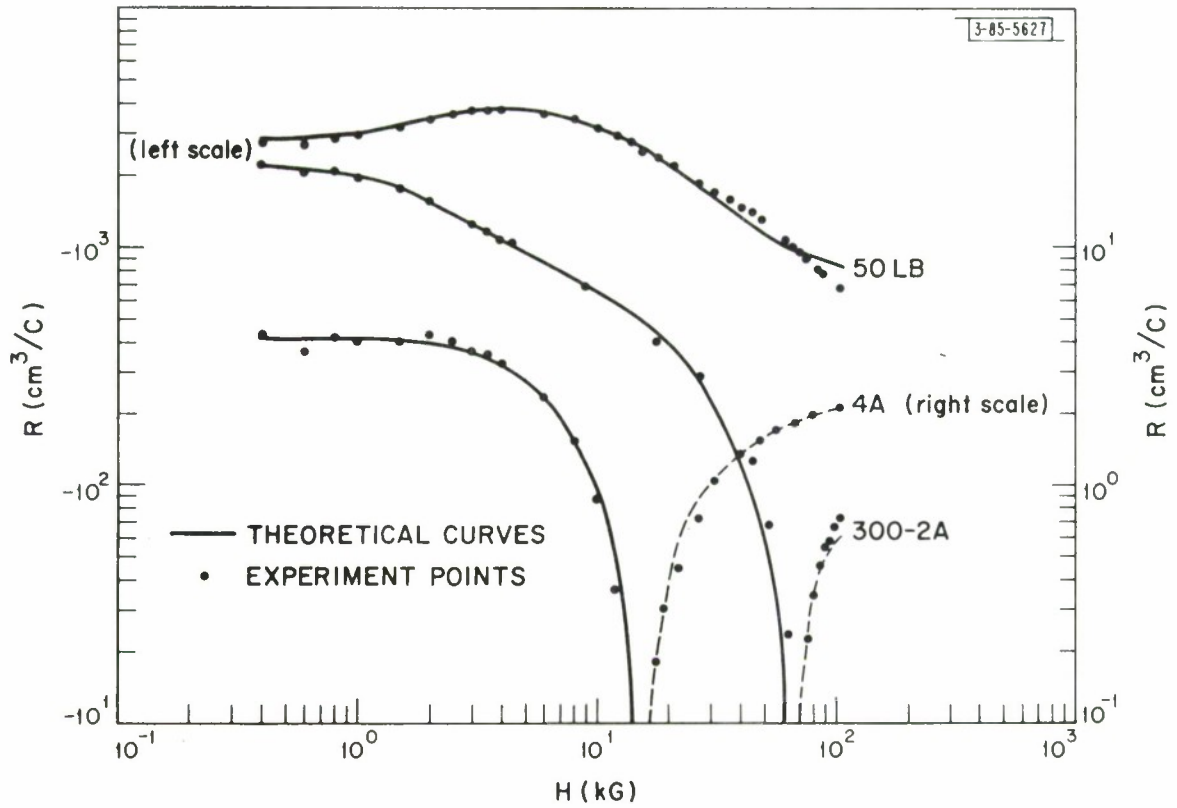


Fig. 2. Theoretical and experimental Hall coefficient of HgTe at 4.2° K. Samples 50 LB, 4-A and 300-2A.

should be noted: (1) The signs for the n_i and μ_i were determined by the computer; from the tabulation one concludes that an optimal fit of the data requires that two of the three carriers be electron-like. (2) A variation of any of the carrier density or mobilities by $\pm 10\%$ about the listed value resulted in a noticeably poorer fit of the theory to the data, as judged from least-squares calculations. This was also the case when one or more of the parameters were simultaneously altered by $\pm 10\%$. The values listed in Table 2 as providing the optimal fit are thus known with reasonable precision.

A comparison between the calculated and the observed magneto-Hall effects is provided in Fig. 2. Correlations between the results of Table 2 and the observations in Fig. 2 are readily apparent: Sample 50 LB exhibits a negative Hall coefficient because the two sets of electrons outweigh the holes in concentration. In passing one should note the distinct maximum (actually, a minimum) in the magneto-Hall curve for this sample; on the basis of elementary arguments it may be shown that this cannot occur in a two-carrier model under the assumption that the one carrier R_i and σ_i are independent of H . In samples 4A and 300-2A the sign reversal of R in passing from low to high magnetic fields reflects the preponderance in concentration of low-mobility holes over intermediate and high-mobility electrons.

As is evident from Fig. 3, there is considerable discrepancy between the calculated and the observed magnetoresistance values,

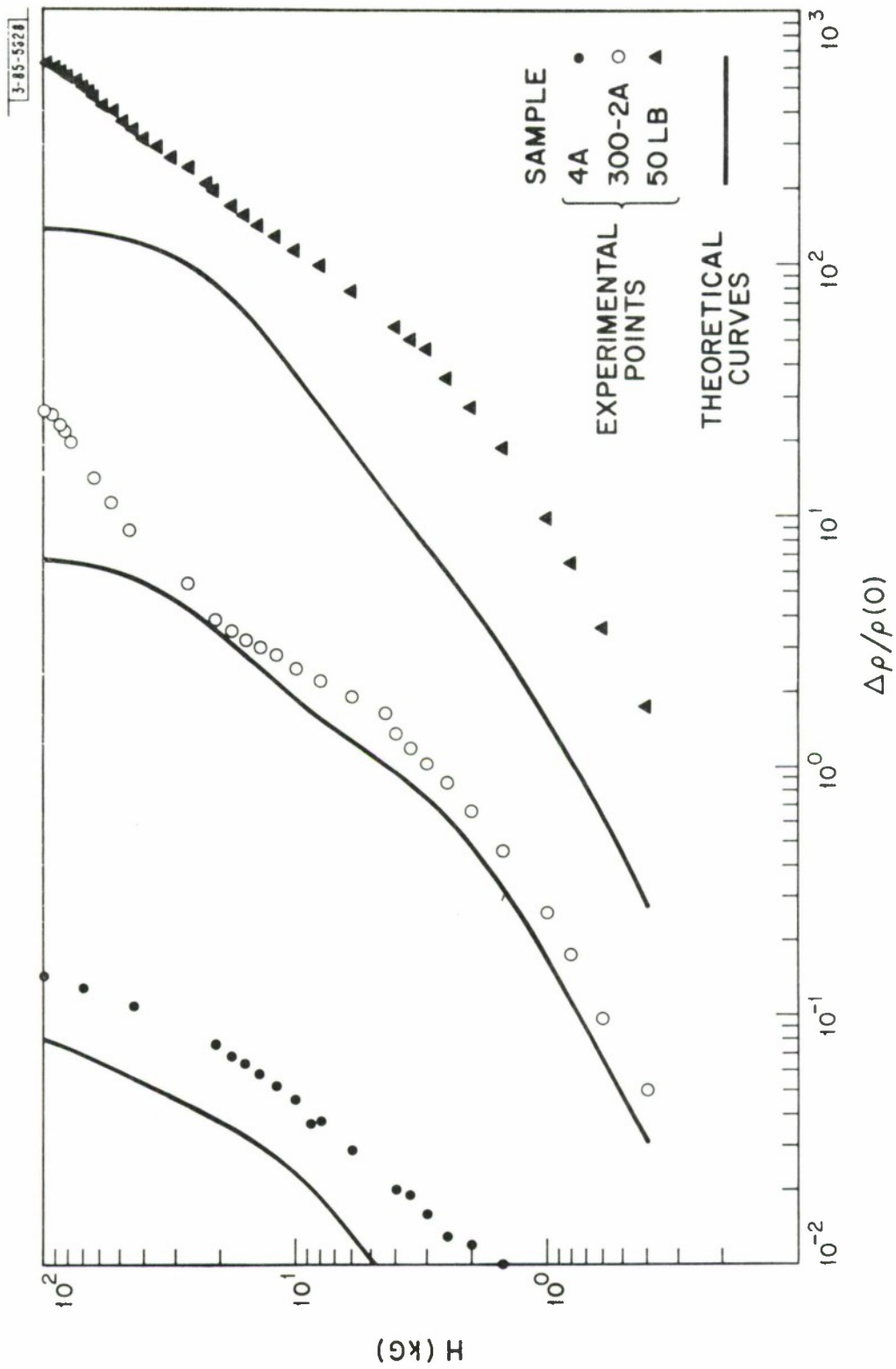


Fig. 3. Theoretical and experimental magnetoresistance of HgTe at 4.2°K. Samples 50LB, 4-A and 300-2A.

although the general trend of the experimental results is correctly brought out in the calculations. The fit could be considerably improved by using both $\mathcal{R}(H_\ell)$ and $\rho(H_\ell)$ as input parameters to the computer program. The discrepancies are due in part to the simplifying assumption which neglects the variation of R_i and σ_i on H . It should be noted that in sample 50 LB the magnetoresistance attained values in excess of 600 without showing any saturation effects at 110 kG.

The results cited above are consistent with the band model sketched in Fig. 1(d). As has been pointed out in Ref. 6, it is generally rather difficult to determine the thermal overlap energy E_t with precision. A lower limit to this quantity is calculated from the value of n_i for sample 50 LB; here, $E_t > E_F$ where E_F is the Fermi level relative to the bottom of the conduction band. Using an effective electron mass of $m/m_0 = 0.023$, as determined from the direct gap⁽¹⁶⁾ energy value of $E_g = 0.283$ eV and from the Kane parameter $\mathcal{Q} = 8.3 \times 10^{-8}$ eV-cm, one finds that

$$E_F = \left(\frac{3n_i}{8\pi} \right)^{2/3} \frac{h^2}{2m} = 0.0028 \text{ eV}; \quad (3)$$

an upper limit⁽⁶⁾ to E_t of 0.02 eV is set by calculations involving the two-band model.

Conclusions

Magneto-Hall and transverse magnetoresistance data on a large number of HgTe single crystals indicate that a three-carrier model involving two sets of electrons and one set of holes should be used in the interpretation of the data. These findings are consistent with an inverted band structure model shown in Fig. 1(d); the lower limit to the overlap energy E_t is 0.0028 eV. An unusually high electron mobility of $640,000 \text{ cm}^2/\text{V-sec}$ was obtained at 4.2°K as a result of special conditions of crystal growth.

Acknowledgment

The authors are grateful to A.E. Paladino and J.R. McNally for their assistance in preparing the materials and for making many of the electrical measurements, and to S. Hilsenrath for performing some calculations. They are also pleased to acknowledge the helpful comments of Dr. J. O. Dimmock and Dr. S. H. Groves.

Finally, they express their appreciation to the National Magnet Laboratory for use of the high magnetic field facilities in carrying out the Hall and resistivity measurements.

Appendix A - The Quartic Band

In this appendix we describe briefly the electrical characteristics to be associated with a quartic band model of the form

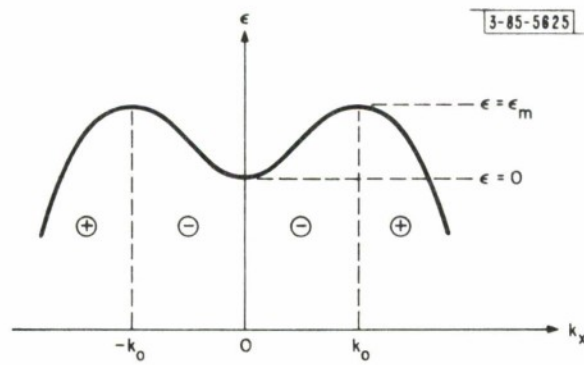
$$\frac{\epsilon}{kT} \equiv x = -A k_r^4 + B k_r^2 \quad (A-1)$$

which is sketched in Fig. 4. Here ϵ is the energy, k is Boltzmann's constant, A and B are constants, and k_r is the radial component of the wave number vector. It is seen that a band of the form (A-1) simulates one of the Γ_8 bands in the proposed band scheme for HgTe, Fig. 1(d).

It is important to note that for such a band with spherical symmetry the current density may be split into two contributions, namely

$$\begin{aligned} \tilde{J} &= \left\{ \int_0^{k_0} + \int_{k_0}^{\infty} \right\} \int_{-\pi/2}^{\pi/2} \int_0^{2\pi} Z e \tilde{v} f_1 k_r^2 \sin\theta \, dk_r \, d\theta \, d\phi \\ &\equiv \tilde{J}_1 + \tilde{J}_2 \end{aligned} \quad (A-2)$$

where e is the electronic charge, $Z = \pm 1$, $\tilde{v} \equiv \hbar^{-1} \nabla_{\tilde{k}} \epsilon$, f_1 the deviation of the nonequilibrium distribution function from the



BAND STRUCTURE CHARACTERIZED

$$\text{BY } \frac{\epsilon}{kT} = x = -Ak^4 + Bk^2$$

Fig. 4. The quartic band structure model.

Fermi-Dirac distribution function $f_0 \equiv [\exp(x-\eta)+1]^{-1}$, η the reduced Fermi level relative to the appropriate band edge; θ_k and ϕ_k are the appropriate angular coordinates in \tilde{k} -space, and quantities \tilde{v} and f_1 are functions of x alone and are thus independent of θ_k, ϕ_k . One may therefore treat the band in Fig. 4 as a combination of two sub-bands, each of which may be considered separately.

Focusing on the inner band, $0 < k_r < k_0$, and switching to the formulation of transport effects in terms of irreversible thermodynamics we now write:

$$J_1^x = \sigma_{xx} V_x + \sigma_{xy} V_y \quad (A-3)$$

$$J_1^y = \sigma_{yx} V_x + \sigma_{yy} V_y \quad (A-4)$$

where $V_\lambda \equiv \nabla_\lambda (\zeta/e)$, ζ being the Fermi level relative to the electron at rest in free space, and where $\sigma_{yx} (-H_z) = \sigma_{xy} (H_z)$, $\sigma_{xx} (H_z^2) = \sigma_{yy} (H_z^2)$ are the components of the conductivity tensor.

Setting $J_1^y = 0$ and eliminating V_y from (A-3) we then obtain
 $(\nabla T = 0, J_1^y = 0)$

$$\mathcal{R}_1 = V_y / J_1^x = \sigma_{yx} / [\sigma_{xy} \sigma_{yx} - \sigma_{xx} \sigma_{yy}] \quad (A-5)$$

As the band under consideration is filled with charge carriers,

thereby increasing k_r from 0 towards k_o , the denominator in (A-5) remains unaltered in sign. The sign of σ_1 is thus determined by that of σ_{yx} . As shown elsewhere⁽²⁰⁾, for bands of spherical symmetry, and for cases where the Boltzmann transport equation in the relaxation time formalism applies,

$$\sigma_{yx} = e^3 \int_0^{k_o} \int_{-\pi/2}^{\pi/2} \int_0^{2\pi} \frac{v_y^2 \omega \tau^2}{1 + \omega^2 \tau^2} \frac{\partial f_o}{\partial \epsilon} k_r^2 \sin \theta_k d k_r d \theta_k d \phi_k \quad (A-6)$$

where τ is the relaxation time, $v_y \equiv \hbar^{-1} \nabla_{k_y} \epsilon$, and where $\omega \equiv -eH_z/m^*c$. The sign of σ_{yx} is thus governed by that of the first derivative effective mass⁽²⁰⁾

$$1/m^* = (1/k_r) (\partial \epsilon / \partial k_r). \quad (A-7)$$

With k_r being the radius vector relative to the origin of coordinates at the point of spherical symmetry, the effective mass, according to (A-1), remains positive for $0 < k_r < k_o$, but is negative for $k_r > k_o$. It follows that insofar as the Hall coefficient is concerned, the inner portion of the band in Fig. 4 is always populated with electron-like carriers, regardless of the degree of filling, while the outer portion of the band in Fig. 4

is populated with holes. It is of interest that a similar argument pertaining to the Seebeck coefficient leads to the conclusion that the thermoelectric power changes sign as the inner band is progressively filled with carriers.

These findings are substantiated by a detailed study in which (A-1) was solved for $Q(x)$ and the results used in the explicit evaluation of transport integrals according to the procedures of Ref. 20.

Appendix B - Optimization Routine

The charge carrier densities and mobilities listed in Table 2 were determined by an optimization routine due to Nelder and Mead. (21) In essence, the program is designed to minimize the function

$$\phi(n_2, n_3, \mu_1, \mu_2, \mu_3) = \sum_{i=1}^K [\mathcal{R}_E(x_i) - \mathcal{R}_T(x_i)]^2 \quad (\text{B-1})$$

where the subscript E and T designate respectively the Hall coefficients determined experimentally and those calculated according to Eq. (2). In Eq. (B-1) the variable n_1 has been eliminated by use of Eq. (1), rewritten as

$$A \equiv n_1\mu_1 + n_2\mu_2 + n_3\mu_3 = 1/e\rho(0) \quad (\text{B-2})$$

The method requires an initial guess of $n_2, n_3, \mu_1, \mu_2, \mu_3$ which locates a point in five-space; the computer then generates five additional points in the vicinity, according to a prescribed routine, and determines the center of gravity of the resulting convex polyhedron in five-space, called a simplex. The function ϕ is then calculated according to Eq. (B-1) for each of the vertices of the simplex; the vertex (extremum) corresponding to the highest ϕ is singled out, and a new point is located at

a prescribed distance along the line passing through the vertex in question and the center of gravity. The old extremum is now discarded, and a new simplex generated from the new point and the remaining vertices of the original simplex. The procedure is repeated until the final simplex consists of six points spaced very closely together. The center of gravity now corresponds to the optimal values of the parameters; however, this set under certain conditions may correspond to a local minimum in ϕ rather than to the true minimum. To guard against this possibility, each of the points of the final simplex is distended in turn by 5 to 10% from its value, and the process of finding a minimum in ϕ is repeated.

The advantage in the approach lies in the fact that it is readily programmed in Fortran, that it is free from erratic loops, and that it does not require programming of the derivatives of ϕ . The total machine time required to run through a set of experimental points on a SDS 930 computer was of the order of five minutes.

REFERENCES

1. T.C. Harman and A. J. Strauss, J. Appl. Phys. Supp. 32, 2265 (1961).
2. A. J. Strauss, T.C. Harman, J. G. Mavroides, D. H. Dickey and M.S. Dresselhaus, Proc. Int. Conf. Physics of Semiconductors, Exeter (Institute of Physics and The Physical Society; London, 1962), p. 703 ff.
3. T.C. Harman, W. H. Kleiner, A. J. Strauss, G.B. Wright, J.G. Mavroides, J. M. Honig and D. H. Dickey, Solid State Comm. 2, 305 (1964).
4. S.Groves and W. Paul, Phys. Rev. Letters 11, 194 (1963); Proc. 7th Int. Conf. Physics of Semiconductors (Dunod, Paris, 1964), p. 41 ff.
5. W. Gorzkowski, Phys. Stat. Sol. 15, K9 (1966).
6. T.C. Harman in Physics and Chemistry of II-VI Compounds, M.Aven and J. S. Prener, eds. (North Holland Publishing Co., Amsterdam, 1967), Chap. XV.
7. V. I. Ivanov-Omskii, B. T. Kolomiets, A.A. Mal'kova, V. K. Ogorodnikov and K. P. Smekalova, Phys. Stat. Sol. 8, 613 (1965).
8. C. Hilsum and R. Barrie, Proc. Phys. Soc. London 71, 676 (1958).
9. R.A. Stradling and G.A. Antcliffe, Proc. 8th Int. Conf. Physics of Semiconductors, Tokyo, 1966 [J. Phys. Soc. Jap. 21, 374 (1966)].
10. R.T. Delves, Proc. Phys. Soc. London 87, 809 (1966).

11. K.D. Tovstyuk, N. P. Gavaleshko and P. M. Rarenko, Izv. Akad. Nauk SSSR, Ser. Fiz. 28, 1048 (1964).
12. E.E. Kolosov and P.V. Sharavskii, Sov. Phys.-Solid State 7, 2973 (1966).
13. C. Verié, Phys. Stat. Sol. 17, 889 (1966).
14. M. Yamamoto and T. Fukuroi, J. Phys. Soc. Japan 21, 2428 (1966).
15. J. M. Honig and T. C. Harman, Adv. Energy Conv. 3, 529 (1963).
16. S. Groves, personal communication.
17. R. K. Willardson, T. C. Harman and A. C. Beer, Phys. Rev. 96, 1512 (1954).
18. A. H. Wilson, "The Theory of Metals" (Cambridge University Press, 2nd, ed., 1958) pp. 236-240.
19. G. Fischer, Helv. Phys. Acta. 33, 463 (1960).
20. T. C. Harman and J. M. Honig, J. Phys. Chem. Solids 23, 913 (1962). T. C. Harman, J. M. Honig and B. M. Tarmy, ibid., 24, 835 (1963).
21. J. A. Nelder and R. Mead, Computer J. 7, 308 (1965).

DOCUMENT CONTROL DATA - R&D		
<i>(Security classification of title, body of abstract and indexing annotation must be entered when the overall report is classified)</i>		
1. ORIGINATING ACTIVITY (Corporate author) Lincoln Laboratory, M. I. T.	2a. REPORT SECURITY CLASSIFICATION Unclassified	
	2b. GROUP None	
3. REPORT TITLE Hall Coefficient and Transverse Magnetoresistance in HgTe at 4.2°K and 77°K		
4. DESCRIPTIVE NOTES (Type of report and inclusive dates) Technical Note		
5. AUTHOR(S) (Last name, first name, initial) Harman, Theodore C. Honig, Jurgen M. Trent, Philip H.		
6. REPORT DATE 25 August 1967	7a. TOTAL NO. OF PAGES 30	7b. NO. OF REFS 21
8a. CONTRACT OR GRANT NO. AF 19(628)-5167	9a. ORIGINATOR'S REPORT NUMBER(S) Technical Note 1967-43	
b. PROJECT NO. 649L	9b. OTHER REPORT NO(S) (Any other numbers that may be assigned this report) ESD-TR-67-484	
c.		
d.		
10. AVAILABILITY/LIMITATION NOTICES This document has been approved for public release and sale; its distribution is unlimited.		
11. SUPPLEMENTARY NOTES None	12. SPONSORING MILITARY ACTIVITY Air Force Systems Command, USAF	
13. ABSTRACT A band structure model is proposed in Fig. 1(d) which is consistent with magneto-Hall and magneto-resistance data obtained for various samples of HgTe at 4.2°K. Using an optimization routine it was ascertained that the data could be fitted on the basis of a three-carrier model involving two sets of electrons and one set of holes. Under special crystal growth conditions the electron Hall mobility at 4.2°K of HgTe exceeded 640,000 cm ² /v-sec.		
14. KEY WORDS Hall coefficient magnetoresistance mercury telluride		